Identification of Different Electron Screening Behavior Between the Bulk and Surface of (Ga,Mn)As

J. Fujii,[1] M. Sperl,[2] S. Ueda,[3] K. Kobayashi,[3] Y. Yamashita,[3] M. Kobata,[3] P. Torelli,[1] F. Borgatti,[4] M. Utz,[2] C. S. Fadley,[5,6]
A. X. Gray,[5,6] G. Monaco,[7] C. H. Back,[2] G. van der Laan,[8] and G. Panaccione[1]

[1]*CNR Istituto Officina dei Materiali (IOM), Laboratorio TASC, S.S.14, Km 163.5, I-34149 Trieste, Italy*
[2]*Institut für Experimentelle Physik, Universität Regensburg, D-93040 Regensburg, Germany*
[3]*NIMS beamline Station at Spring-8, National Institute for Materials Science, Sayo, Hyogo 679-5148, Japan*
[4]*CNR Istituto per lo Studio dei Materiali Nanostrutturati (ISMN), via P. Gobetti 101, I-40129 Bologna, Italy*
[5]*Department of Physics, University of California, Davis, California 95616, USA*
[6]*Material Sciences Division, Lawrence Berkeley National Laboratory, Berkeley, California 94720, USA*
[7]*European Synchrotron Radiation Facility (ESRF), BP 220, F-38043 Grenoble, France*
[8]*Diamond Light Source, Chilton, Didcot, Oxfordshire OX11 0DE, United Kingdom*
(Received 25 July 2011; published 27 October 2011)

We report x-ray photoemission spectroscopy results on (Ga,Mn)As films as a function of both temperature and Mn doping. Analysis of Mn $2p$ core level spectra reveals the presence of a distinct electronic screening channel in the bulk, hitherto undetected in more surface sensitive analysis. Comparison with model calculations identifies the character of the Mn $3d$ electronic states and clarifies the role, and the difference between surface and bulk, of hybridization in mediating the ferromagnetic coupling in (Ga,Mn)As.

The extensive effort in understanding the mechanisms at the origin of ferromagnetic order in diluted magnetic semiconductors (DMS) has resulted in a wealth of new concepts in spintronics [1–4]. In the case of (Ga,Mn)As—the prime representative of a DMS material—recent advances have demonstrated that the properties of the first few atomic layers play a fundamental role for possible spintronics applications [5,6]. Manipulation of the carrier density, and consequently of the magnetic properties, has been demonstrated via electrical gating [7,8]. Efficient spin injection from (Ga,Mn)As into GaAs and room temperature ferromagnetism of thin layers of (Ga,Mn)As have been achieved in engineered heterostructures [9] or in hybrid structures comprised of ferromagnetic overlayers grown on DMS [10,11]. Although many experimental and theoretical efforts have been focused on reaching a reliable control and description of surface and interface effects of (Ga,Mn)As, a basic understanding of the differences between surface and bulk electronic properties is still lacking [12–14] and fundamental open questions persist regarding the spatial homogeneity of the coupling between Mn ions and the role, understanding, and control of the reduced carrier density at interfaces [7]. A meaningful experimental investigation of these important properties requires, on the one hand, the ability to probe the electronic and magnetic properties with chemical sensitivity, and, on the other hand, an adequate control over the depth information. Photoemission spectroscopy (PES), and, in particular, x-ray based PES, is a powerful method that possesses these prerequisites. Reports of PES on DMS, however, are scarce [15,16], which is mainly due to the extreme

surface sensitivity of this technique, which in turns requires surface preparation methods, often producing a severe modification of the surface and interface electronic properties [17,18].

Here we report on high resolution hard x-ray PES (HAXPES) data obtained on (Ga,Mn)As films. Owing to the unusually high achievable bulk sensitivity, with probing depth ≥ 100 Å, we are able to deduce striking differences in electron screening between surface and bulk. We observe the presence of extra features in the Mn $2p$ core level spectra: using model calculations, we can ascribe these changes to the electron screening process, which highlights the importance of the d-electron hybridization with respect to the ferromagnetic properties. Mn $2p$ HAXPES spectra vs temperature and vs Mn doping reveal details of the carrier properties in terms of localized vs itinerant behavior.

The ferromagnetic (Ga,Mn)As films (Mn 1%, 5%, and 13% doping with 50, 35, and 18 nm of thickness, respectively) were grown by molecular beam epitaxy using a modified Veeco Gen II system. A description of the (Ga,Mn)As sample growth, preparation, and characterization is found in Refs. [18,19]. For the present experiment, contamination free surfaces were obtained by HCl etching [17]. The magnetic characterization, before and after the chemical etching procedure, was performed using x-ray magnetic circular dichroism, superconducting quantum interference device magnetometry, and magneto-optical Kerr effect on pieces of the very same samples, revealing (i) the complete removal of Mn oxide from the surface after chemical etching, and (ii) stable long-range ferromagnetic

order with $T_c \lesssim 4$, 60, and 80 K for 1%, 5%, and 13% Mn doping, respectively. Post-annealing of the sample has been purposely avoided, in order to exclude MnAs cluster segregation on the surface. HAXPES measurements were carried out using linearly polarized synchrotron radiation at SPring-8 (beamline BL15XU) [20], and at the ESRF (beamline ID16, with VOLPE spectrometer) [21]. The overall energy resolution was set to 250 meV (SPring-8) and 400 meV (ESRF). Configuration interaction in the initial and final states is taken into account using an Anderson impurity model [22,23]. We consider a particular Mn site in a cluster of other atoms with a basis set of states $3d^n$ ($n = 3, 4, 5, 6, 7$) and holes h, with a combination of appropriate symmetry of states characterizing a As p—Mn d hybridized valence band hole. X-ray photoemission excites a core electron to a continuum state ε, where the electrostatic and spin-orbit interactions of the continuum electron are taken equal to zero. The Mn ground state is a mixture of the configurations d^n, and the final states of $\underline{c}d^n\varepsilon$, also mixed by hybridization. The Hamiltonians for the initial and final states of the Mn atoms were calculated using Cowan's code including tetrahedral crystal-field symmetry ($10Dq = -0.5$ eV) and multiplet structure but neglecting band structure dispersion. The code calculates the wave functions in intermediate coupling using the atomic Hartree-Fock approximation with relativistic corrections. The Slater parameters were reduced to 80%, to account for the effects of intra-atomic correlation. Cluster parameter values, as used for Fig. 1 and Table I, were as follows: the charge-transfer energy, $\Delta = E(d^6) - E(d^5) = 1$ eV, the intra-atomic Coulomb interaction, $U = 4$ eV, and the core-valence Coulomb interaction, $Q = 5$ eV. This gives the energy positions before hybridization in the initial state as $E(d^4) = -\Delta + U = 3$ eV, $E(d^5) = 0$ eV, and $E(d^6) = \Delta = 1$ eV, and in the final state as $E(\underline{c}d^4) = -\Delta + U + Q = 8$ eV, $E(\underline{c}d^5) = 0$ eV, and $E(\underline{c}d^6) = \Delta - Q = -4$ eV.

Figure 1(a) compares the Mn $2p$ photoemission spectra from the same (Ga,Mn)As film (5% Mn, $T_c = 60$ K), after HCl chemical etching, measured using soft and hard x-ray energies. These spectra correspond to inelastic mean free path of ~ 8 Å (soft x ray), and ~ 50 Å (hard x ray), as calculated using the TPP-2M approximation for GaAs [24]. More quantitatively, theoretical calculations and experimental results indicate an information depth of ≈ 150 Å for the HAXPES regime, while for soft x rays it is limited to ≈ 30 Å [25]. The surface sensitive spectrum agrees well with previous Mn $2p$ PES reports in which the main $2p_{3/2}$ and $2p_{1/2}$ peaks are accompanied by broad features at higher binding energy (BE) [15]. In contrast, the Mn $2p$ HAXPES spectrum reveals an additional sharp feature at the onset of the main $2p_{3/2}$ peak [marked by the dashed line in Fig. 1(a)], which is completely absent in the surface sensitive PES. Its energy position agrees well with previous HAXPES results on (Ga,Mn)As, but the
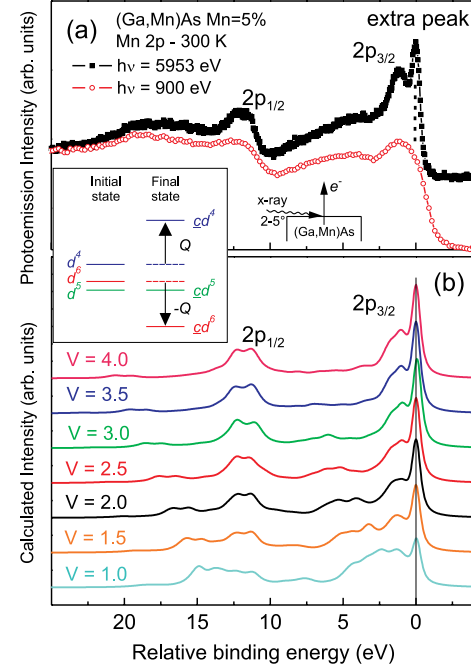

FIG. 1 (color online). (a) Mn $2p$ PES of (Ga,Mn)As (5% Mn) after HCl chemical etching. The overall energy resolution was set to 250 meV ($h\nu = 900$ eV) and 400 meV ($h\nu = 5953$ eV). Spectra have been aligned to the same relative BE scale without background subtraction. (b) Calculated evolution of the Mn $2p$ HAXPES spectral features as a function of the hybridization parameter V. Spectra (offset for clarity) are convoluted with a Lorentzian [$\Gamma = 0.25$ eV (leading peak), 0.5 eV (rest)] and Gaussian ($\sigma = 0.15$ eV) to account for lifetime and experimental resolution, respectively. Inset: energy level diagram of the d states in the initial and final state before hybridization and without crystal-field and multiplet structure.

energy resolution in the present spectra is considerably better and the sharp feature more easily visible [26]. Similar low-BE peaks have recently been reported in HAXPES from $3d$-based transition metal oxides, and are referred to as well-screened peaks; they are generally associated with a metalliclike, i.e., delocalized, character [27–30]. We have simulated the PES process using the cluster model (a local ligand state version of the

TABLE I. Calculated ground state $3d$ weights (in %) of Mn atoms vs hybridization parameter V (in eV). In bold, the d^6 configuration, responsible for the observed extra peak in Mn $2p$ HAXPES.

V	d^3	d^4	d^5	d^6	d^7	d-count	st dev
4.0	0.8	13.7	47.5	**32.5**	5.5	5.28	0.795
3.0	0.4	11.8	54.5	**29.6**	3.6	5.24	0.718
2.5	0.3	10.0	60.8	**26.5**	2.8	5.24	0.666
2.0	0.1	7.4	69.5	**21.6**	1.4	5.17	0.567
1.5	0.0	4.5	80.1	**14.8**	0.6	5.12	0.451
1.0	0.0	2.0	90.2	**7.2**	0.1	5.05	0.311

Anderson impurity model) [22,23]. The energy of each possible final state depends on how effective the core hole is screened by the valence electrons. The inset in Fig. 1 shows the schematic energy level diagram for the Mn 3d configurations in (Ga,Mn)As in the initial and final states of the PES process in the absence of hybridization ($V = 0$) and without multiplet structure. In the initial state, $d^5\underline{h}$ is the lowest configuration, but with significant mixing of d^4 and $d^6\underline{h}^2$, where $\underline{h}$ denotes a combination of appropriate symmetry of states characterizing a hybridized valence band hole near the Fermi level. Although the d^5 and d^6 configurations are close in average energies, the lowest energy levels in the initial state are mainly d^5 because the multiplet structure is much broader for d^5. In the final states, the $\underline{c}d^6\underline{h}^2$ configuration, where c denotes the core hole, is pulled down in energy (i.e., towards lower BE) by an amount Q due to the core-valence Coulomb interaction compared to the $\underline{c}d^5\underline{h}$ configuration. An essential point to note is that the relative energy positions of the d^5 and d^6 configurations are reversed in the final states compared to the initial state. Turning on the hybridization between the configurations, the $\underline{c}d^5$ peak increases in intensity. Thus this low-BE peak corresponds to the well-screened state, which has an extra d electron. Figure 1(b) shows the calculated Mn 2p PES for different V. Keeping the energies of the d levels fixed, V was varied between 1 and 4 eV. For large hybridization the spectrum reflects mainly $\underline{c}d^6$ final states. Upon decreasing the hybridization, the $\underline{c}d^5$-like final states, seen up to 6 eV above the main peak, strongly gain in relative intensity. By comparing the calculations with the experimental data in Fig. 1(a), we are now able to unambiguously assign the extra peak at the low-BE side of the Mn 2p HAXPES spectrum to the well-screened $\underline{c}d^6$-like peak, whereas the broader peak at 1–2 eV higher BE is the well-screened peak which is a mixture of $\underline{c}d^6$ and $\underline{c}d^5$ final states, which in addition shows multiplet structure. The experimental HAXPES spectra agree best with a mixing of $V \approx 2.5$ eV. The absence of the well-screened peak in the low photon energy PES spectrum of Fig. 1(a), and by implication a small value of V, indicates a more localized electronic environment in the vicinity of the surface. This finding is in full agreement with the results presented in Ref. [7] where it was shown that a significant carrier depletion layer exists at the surface of (Ga,Mn)As. For the given values of Δ and U the multiplet calculations with different V give the d^n weights in the initial state, as shown in Table I. The meaning of the hybridization parameter V becomes clear from the corresponding d^n weights (in %); e.g., a larger V results in a broader spread over the d levels.

Figure 2 shows the Mn 2p HAXPES spectra of (Ga,Mn)As (13% Mn, $T_c = 80$ K) vs temperature. One observes that the relative intensity of the well-screened peak compared to the poorly-screened peak increases significantly for a temperature below T_c. The redistribution of spectral
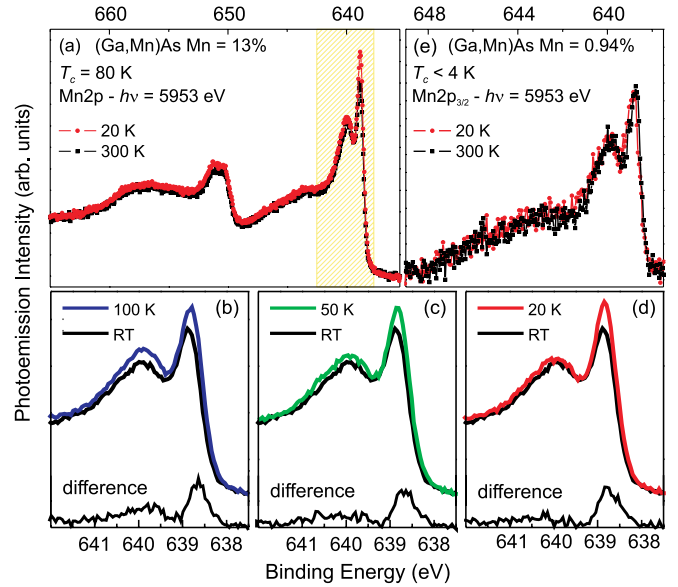

FIG. 2 (color online).   (a) Mn 2p HAXPES spectra of (Ga,Mn)As (13% Mn, $T_c = 80$ K) vs temperature. (b)–(d) Expanded view of the 2$p_{3/2}$ region, showing the difference of the spectra at room temperature with those at low temperatures. Spectra have been normalized at the background as in panel (a). The intensity of the well-screened peak increases when lowering the temperature. (e) Mn 2$p_{3/2}$ HAXPES spectra of (Ga,Mn)As (1% Mn, $T_c \leq 4$ K) measured at room temperature (squares) and at $T = 20$ K (circles). No significant change in intensity and/or redistribution of spectral weight is observed.

weight is better seen in Figs. 2(b)–2(d), where the differences between three low temperature spectra (100, 50, 20 K) and the room temperature one are shown, in the Mn 2$p_{3/2}$-spectral region. One observes a clear redistribution of spectral weight, where the intensity of the well-screened peak increases when lowering the temperature while the peak located around BE ≈ 640 eV looses spectral weight. From the comparison between experiments and calculations we are able to clarify that (i) a higher relative intensity of the well-screened peak means a larger hybridization, i.e., the Mn d states become less localized, and (ii) a change in hybridization and a redistribution of the d weight in the electron screening is observed upon crossing T_c; i.e., the hybridization increases when ferromagnetic order settles in (Ga,Mn)As. The one-to-one correspondence between the intensity change of the well-screened peak and the collective electronic behavior is confirmed in Fig. 2(e), where Mn 2p HAXPES spectra from a (Ga,Mn)As sample with 1% Mn doping are compared vs temperature. In this case $T_c \leq 4$ K, and within our detection limit, no intensity change is observed down to 20 K. This suggests further that the hybridized d^6 electronic character is mainly responsible for mediating the ferromagnetic coupling among the localized substitutional Mn atoms.

The difference in the screening ability between surface and bulk is schematically illustrated in Fig. 3, where in
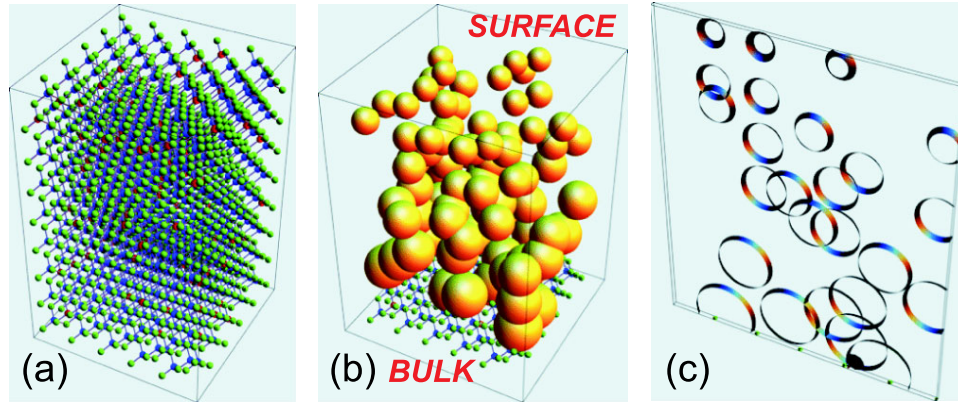
FIG. 3 (color online). (a) The GaAs zinc blende structure with randomly substituted Mn atoms on the Ga sites. (b) The electronic clouds of partially localized Mn d electrons are approximated by spheres, with a radius proportional to the screening length. Near the surface (top side) the d electrons are more localized (smaller radius) than in the bulk (bottom side, larger radius). (c) 2D cross section of panel b: only in the bulk the d electrons can percolate through the lattice, favoring long-range ferromagnetism.

panel (a) we present the zinc blende structure of GaAs with randomly substituted (10%) Mn atoms on the Ga sites. Each Mn atom carries a cloud of partially localized d electrons, represented as yellow spheres in panel (b). A difference in the spatial extension of the electronic cloud at the surface and in the bulk, as derived by the calculation, is obtained for different screening length (hybridization): near the surface (top side) the d electrons are more localized than in the bulk (bottom side), which is indicated by a smaller (larger) radius of the spheres. In panel (c), a cross section of panel (b) shows that only in the bulk will the d electrons percolate through the lattice; i.e., a sizeable overlapping of electronic clouds is found, giving rise to long-range ferromagnetic ordering below T_c.

In conclusion, we have performed bulk sensitive PES of the Mn $2p$ core level of (Ga,Mn)As: the presence of a strong feature at the low-BE side of the $2p_{3/2}$ peak reveals that the electronic structure of the bulk and the surface of (Ga,Mn)As are profoundly different. This feature shows a noticeable increase for temperatures below T_c and is strongly related to the ferromagnetic phase of (Ga,Mn) As. Anderson impurity model calculations establish electron screening as its origin, which is strongly suppressed close to the surface. This result is expected to help to understand and to control the electronic and magnetic surface properties of (Ga,Mn)As, which are of importance in spintronics applications.

[1] D. D. Awschalom and M. E. Flattè, Nature Phys. **3**, 153 (2007).
[2] H. Ohno et al., Nature (London) **408**, 944 (2000).
[3] T. Dietl, Nature Mater. **9**, 965 (2010).
[4] A. H. Macdonald, P. Schiffer, and N. Samarth, Nature Mater. **4**, 195 (2005).
[5] I. Zutic, J. Fabian, and S. Das Sarma, Rev. Mod. Phys. **76**, 323 (2004).
[6] C. Chappert, A. Fert, and F. Nguyen Van Dau, Nature Mater. **6**, 813 (2007).
[7] M. Sawicki et al., Nature Phys. **6**, 22 (2009).
[8] D. Chiba et al., Nature (London) **455**, 515 (2008); D. Chiba et al., Science **301**, 943 (2003).
[9] M. Ciorga et al., Phys. Rev. B **79**, 165321 (2009).
[10] F. Maccherozzi et al., Phys. Rev. Lett. **101**, 267201 (2008).
[11] S. Mark et al., Phys. Rev. Lett. **103**, 017204 (2009).
[12] S. S. Dunsinger et al., Nature Mater. **9**, 299 (2010).
[13] S. Ohya et al., Nature Phys. **7**, 342 (2011).
[14] K. W. Edmonds et al., Phys. Rev. Lett. **92**, 037201 (2004).
[15] J. Okabayashi et al., Phys. Rev. B **58**, R4211 (1998).
[16] J. Okabayashi et al., Phys. Rev. B **64**, 125304 (2001).
[17] K. W. Edmonds et al., Appl. Phys. Lett. **84**, 4065 (2004).
[18] F. Maccherozzi et al., Phys. Rev. B **74**, 104421 (2006).
[19] U. Wurstbauer et al., Appl. Phys. Lett. **92**, 102506 (2008).
[20] S. Ueda et al., AIP Conf. Proc. **1234**, 403 (2010).
[21] P. Torelli et al., Rev. Sci. Instrum. **76**, 023909 (2005).
[22] G. van der Laan, S. S. Dhesi, and E. Dudzik, Phys. Rev. B **61**, 12277 (2000).
[23] G. van der Laan and M. Taguchi, Phys. Rev. B **82**, 045114 (2010).
[24] S. Tanuma, C. J. Powell, and D. R. Penn, Surf. Interface Anal. **43**, 689 (2011); S. Tougaard, QUASES-IMFP-TPP2M Version 2.2, http://www.quases.com/ (2002).
[25] M. Sacchi et al., Phys. Rev. B **71**, 155117 (2005).
[26] B. Schmid et al., Phys. Rev. B **78**, 075319 (2008).
[27] K. Horiba et al., Phys. Rev. Lett. **93**, 236401 (2004).
[28] G. Panaccione et al., Phys. Rev. Lett. **97**, 116401 (2006).
[29] S. Ueda et al., Phys. Rev. B **80**, 092402 (2009).
[30] A. K. Shukla et al., Phys. Rev. B **75**, 235419 (2007).